

Functionalization and Kinetic Stabilization of the [4]Paracyclophane System and Aromaticity of Its Extremely Bent Benzene Ring

Takashi Tsuji,* Masahiro Okuyama, Masakazu Ohkita, Hidetoshi Kawai, and
Takanori Suzuki

Contribution from the Division of Chemistry, Graduate School of Science, Hokkaido University,
Sapporo 060-0810, Japan

Received September 23, 2002; E-mail: tsuji@sci.hokudai.ac.jp

Abstract: Kinetic stabilization of the [4]paracyclophane skeleton by the introduction of substituents, which serve to sterically hinder reactions at the reactive bridgehead sites, and properties of the resultant [4]-paracyclophanes are investigated in this study. Modification of the property of [4]paracyclophane by functionalization is also intended. [4]Paracyclophanes are designed to be derived from the corresponding Dewar benzene isomers via their photochemical aromatization, and the requisite 1,4-bridged Dewar benzenes bearing sterically demanding functional groups are prepared. Irradiation of these precursors under matrix isolation at 77 K leads to the formation of [4]paracyclophanes, which exhibit characteristic electronic absorption spectra. The half-lives of the generated species vary widely from less than 1 min at $-90\text{ }^{\circ}\text{C}$ to 0.5 h at $-20\text{ }^{\circ}\text{C}$, depending on the type of substituents and the pattern of substitution. One of the derivatives, **24**, is stable enough and its content in the irradiated mixture is high enough to permit the measurement of the ^1H NMR spectrum. The recorded spectrum, which is reproduced very well by theoretical calculations using the GIAO method at the hybrid HF-DFT (B3LYP/6-31+G*) level, suggests the sustenance of rather strong diatropicity in its severely bent benzene moiety. Calculations on the bent benzene whose geometry is constrained to that calculated for **24** support that aromaticity is retained to a significant extent as compared to that of planar benzene, as judged by the magnetic criteria of aromaticity, that is, diamagnetic susceptibility exaltation and nucleus-independent chemical shift. The reason for the retention of aromaticity despite the severe bending of the benzene ring is discussed. Cyclophane **24** is so strained that it exceeds the corresponding Dewar benzene precursor in energy and thermally reverts to the latter with a half-life of 15 ± 5 min at $-20\text{ }^{\circ}\text{C}$ ($\Delta G^{\ddagger} = 18.3 \pm 0.3\text{ kcal mol}^{-1}$).

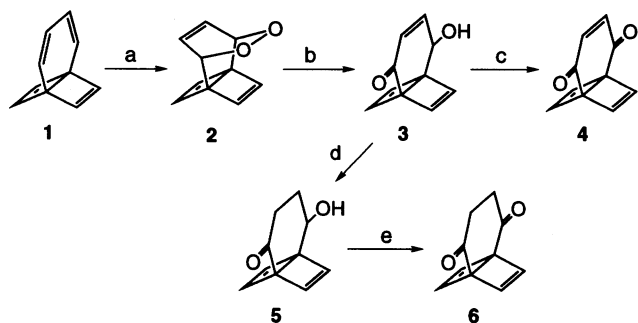
Introduction

The research on the preparation of paracyclophanes with ever shorter bridges has made remarkable progress in the past three decades¹ and has been driven by the interest in the properties of strained molecules and culminated in the successful generation of [4]paracyclophane.^{2,3} [4]Paracyclophane is, however, a highly labile species, rapidly decaying in fluid solution even below $-130\text{ }^{\circ}\text{C}$,³ and the experimental exploration of its properties has been impeded because of the instability. Several theoretical studies of [4]paracyclophane have been conducted,

initially with semiempirical methods⁴ and later by ab initio computations,^{5,6} along with the experimental investigations. Grimme has suggested, on the basis of a high-level ab initio study, that [4]paracyclophane is best classified as a strained molecule with partial diradicaloid character.⁵ He has also pointed out that (i) the small degree of bond alternation in the distorted benzene ring and the benzene-type excited state shows that some benzene-like character is retained, (ii) the strain energy is estimated to be 91 kcal mol^{-1} , and the largest contribution (87%) arises from the deformation of the benzene skeleton, and (iii) the energy difference between [4]paracyclophane and the corresponding Dewar benzene isomer is estimated to be $0 \pm 3\text{ kcal mol}^{-1}$. More recently, Schaefer and co-workers have performed a theoretical investigation on the energetics and magnetic susceptibility of [4]paracyclophane and the related species.⁶ [4]Paracyclophane is now predicted to lie $9 \pm 4\text{ kcal mol}^{-1}$ higher in energy than the Dewar benzene isomer, and

- (1) (a) Bickelhaupt, F.; de Wolf, W. H. *Recl. Trav. Chim. Pays-Bas* **1988**, *107*, 459–478. (b) Bickelhaupt, F.; de Wolf, W. H. In *Advances in Strain in Organic Chemistry*; Halton, B., Ed.; JAI Press: Greenwich, CT, 1993; Vol. 3, pp 185–227. (c) Tobe, Y. In *Topics in Current Chemistry*; Weber, E., Ed.; Springer: Berlin, 1994; Vol. 172, pp 1–40. (d) Kane, V. V.; de Wolf, W. H.; Bickelhaupt, F. *Tetrahedron* **1994**, *50*, 4575–4622. (e) de Meijere, A.; König, B. *Synlett* **1997**, 1221–1232. (f) Tsuji, T. In *Advances in Strained and Interesting Organic Molecules*; Halton, B., Ed.; JAI Press: Stamford, CT, 1999; Vol. 7, pp 103–152. (g) Tsuji, T.; Ohkita, M.; Kawai, H. *Bull. Chem. Soc. Jpn.* **2002**, *75*, 415–433.
- (2) (a) Kostermans, G. B. M.; Bobeldijk, M.; De Wolf, W. H.; Bickelhaupt, F. *J. Am. Chem. Soc.* **1987**, *109*, 2471–2475. (b) Bickelhaupt, F. *Pure Appl. Chem.* **1990**, *62*, 373–382.
- (3) (a) Tsuji, T.; Nishida, S. *J. Chem. Soc., Chem. Commun.* **1987**, 1189–1190. (b) Tsuji, T.; Nishida, S. *J. Am. Chem. Soc.* **1988**, *110*, 2157–2164. (c) Tsuji, T.; Nishida, S. *J. Am. Chem. Soc.* **1989**, *111*, 368–369. (d) Tsuji, T.; Nishida, S.; Okuyama, M.; Osawa, E. *J. Am. Chem. Soc.* **1995**, *117*, 9804–9813.

- (4) (a) Kostermans, G. B. M.; Kwakman, P. J.; Pouwels, P. J. W.; Somsen, G.; de Wolf, W. H.; Bickelhaupt, F. *J. Phys. Org. Chem.* **1989**, *2*, 331–348. (b) Jenneskens, L. W.; Louwen, J. N.; de Wolf, W. H.; Bickelhaupt, F. *J. Phys. Org. Chem.* **1990**, *3*, 295–300. (c) Bockisch, F.; Rayez, J. C.; Liotard, D.; Duguay, B. *J. Comput. Chem.* **1992**, *13*, 1047–1056.
- (5) Grimme, S. *J. Am. Chem. Soc.* **1992**, *114*, 10542–10547.
- (6) Ma, B.; Sulzbach, H. M.; Remington, R. B.; Schaefer, H. F., III. *J. Am. Chem. Soc.* **1995**, *117*, 8392–8400.

Scheme 1^a

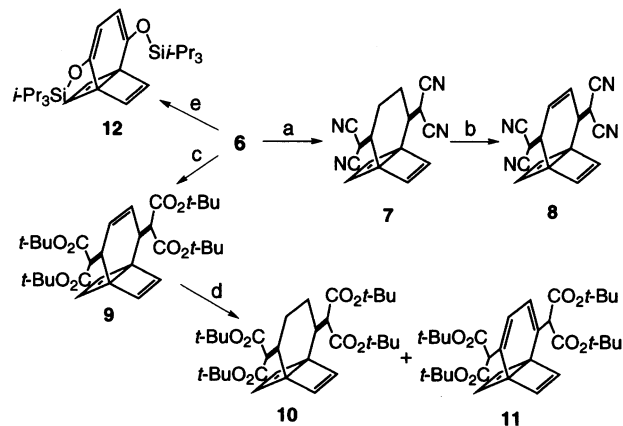
^a (a) $h\nu$ /TPP/ CCl_4 , O_2 , 95%; (b) $\text{Et}_3\text{N}/\text{CH}_2\text{Cl}_2$, 95%; (c) MnO_2 , 92%; (d) Bu_3SnH , $\text{Ph}(\text{PPh}_3)_4$, 84%; (e) PCC, 89%.

the activation energy for the isomerization of the former to the latter is estimated to be 22 kcal mol⁻¹. They also showed that boat-shaped benzene with the same geometry as in [4]paracyclophane has the same magnetic susceptibility as hypothetical cyclohexatriene with alternating double and single bonds, and, therefore, a weak ring current is expected.

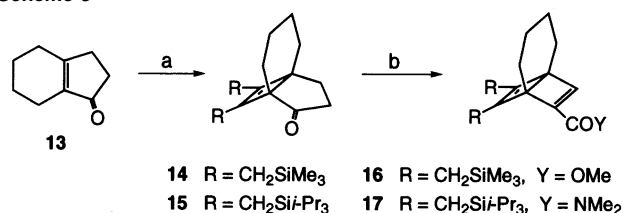
Steric strain in [4]paracyclophane mainly arises from the deformation of the benzene skeleton, as pointed out in those theoretical investigations, and its known reactivity suggests that the extreme lability arises from the susceptibility of bridgehead carbon atoms toward the addition of diverse reagents.^{2,3} This implies that the system may be kinetically stabilized by introducing substituents that specifically shield the bridgehead carbon atoms from access by other reagents. A number of substituted [4]paracyclophanes were designed on the basis of such consideration, and their generation and kinetic stabilities were investigated in this study. One of the derivatives was stable enough to permit the measurement of the ¹H NMR spectrum for the first time for [4]paracyclophane, which suggested the sustenance of a significant diamagnetic ring current in its extremely bent benzene ring. In this paper, we present details of the investigation including (i) the preparation of 1,4-bridged Dewar benzenes bearing a variety of sterically demanding functional groups which serve to hinder reactions at the bridgehead carbon atoms, (ii) their photochemical transformation into the corresponding [4]paracyclophanes, which exhibit characteristic electronic absorption spectra, (iii) degrees of kinetic stability of the resultant [4]paracyclophanes, (iv) successful measurement of the ¹H NMR spectrum of one of the [4]paracyclophanes, (v) theoretical investigation on the aromaticity of [4]paracyclophane, and (vi) experimental verification for the reversal of stability order, benzene form > Dewar benzene form, in [4]paracyclophane.⁷

Results and Discussion

Preparation of 1,4-Bridged Dewar Benzenes Bearing Functional Groups. The generation of functionalized [4]paracyclophanes herein studied was achieved exclusively by the photochemical aromatization of the corresponding Dewar benzene derivatives. The preparation of **4**, **6–10**, and **12** was accomplished through the transformation starting from tetraene **1**^{3d,8} as illustrated in Schemes 1 and 2. Thus, the [2 + 4] cycloadd-

Scheme 2^a

^a (a) $\text{CH}_2(\text{CN})_2$, β -alanine, 54%; (b) $\text{C}_5\text{H}_5\text{N}\cdot\text{HBr}_3/\text{C}_5\text{H}_5\text{N}$, 73%; (c) $\text{CH}_2(\text{CO}_2t\text{-Bu})_2$, $\text{TiCl}_4/\text{C}_5\text{H}_5\text{N}$, 26%; (d) Zn/AcOH , 76% (**10**:**11** = 1:3); (e) $i\text{-Pr}_3\text{SiOTf}/i\text{-Pr}_2\text{NEt}$, 82%.

Scheme 3^a

^a **16**: (a) $h\nu$, 1,4-bis(trimethylsilyl)-2-butyne, 18%; (b) HCO_2Et , EtONa ; TsN_3 , Et_3N , 58%; $h\nu$, MeOH , 80%; LDA , $\text{PhSeBr}/\text{HMPA}$, 79%; H_2O_2 , 53%. **17**: (a) $h\nu$, 1,4-bis(tri-*i*-propylsilyl)-2-butyne, 3%; (b) HCO_2Et , EtONa ; TsN_3 , Et_3N , 55%; $h\nu$, Me_2NH , 66%; LDA , $\text{PhSeBr}/\text{HMPA}$, 31%; $m\text{CPBA}$, 60%.

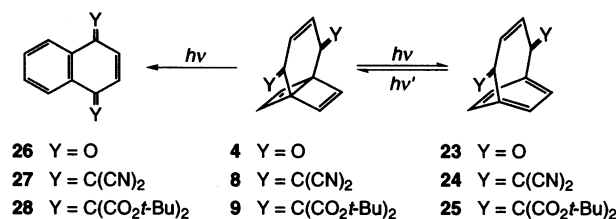
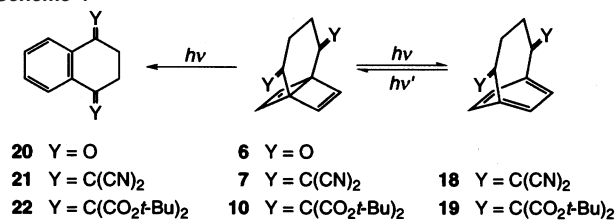
dition of photochemically generated singlet oxygen^{9,10} to **1** smoothly proceeded to afford **2** as colorless crystals in high yield, which provided **3** upon subsequent treatment with triethylamine.⁹ Oxidation of **3** with manganese dioxide in dichloromethane delivered the ene dione derivative **4**, while the chemoselective reduction of the enone moiety of **3**¹¹ followed by PCC oxidation furnished **6**. The Knoevenagel condensation of **6** with malononitrile readily proceeded in the presence of β -alanine¹² to afford **7**, from which **8** was obtained via treatment with pyridinium bromide perbromide in pyridine. The condensation of **6** with di-*tert*-butyl malonate was more difficult but somehow proceeded under the catalysis of TiCl_4 in pyridine to produce **9** directly in reasonable yield.¹³ Reduction of **9** with zinc in acetic acid¹⁴ provided **10** as a minor product, together with **11**. Treatment of **6** with tri-*i*-propylsilyl triflate in *i*-Pr₂NEt furnished the corresponding bis(enol silyl ether) **12**. On the other hand, the Dewar benzene precursors **16** and **17** were prepared from tetrahydroindanone **13** following essentially the same procedure as that reported for the preparation of the corresponding unsubstituted ester,^{3b,8} except that 1,4-bis(trialkylsilyl)but-2-yne were used in place of acetylene (Scheme 3).

- (9) (a) Sütbeyaz, Y.; Seçen, H.; Balci, M. *J. Chem. Soc., Chem. Commun.* **1988**, 1330–1331. (b) Wasserman, H. H.; Murray, R. W. *Singlet Oxygen*; Academic Press: New York, 1979.
(10) Foster, C. H.; Berchtold, G. A. *J. Org. Chem.* **1975**, *40*, 3743–3746 and references cited therein.
(11) Keinan, E.; Gleize, P. A. *Tetrahedron Lett.* **1982**, *23*, 477–480.
(12) Crawford, R. J. *J. Org. Chem.* **1983**, *48*, 1366–1368.
(13) (a) Lehnert, W. *Tetrahedron Lett.* **1970**, 4723–4724. (b) Iio, H.; Isobe, M.; Kawai, T.; Goto, T. *J. Am. Chem. Soc.* **1979**, *101*, 6076–6081.
(14) Elks, J.; Evans, R. M.; Long, A. G.; Thomas, G. H. *J. Chem. Soc.* **1954**, 451–462.

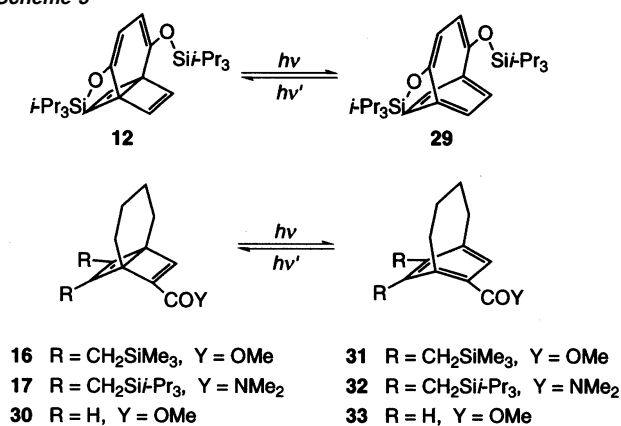
(7) For a preliminary account of this work, see: (a) Okuyama, M.; Tsuji, T. *Angew. Chem., Int. Ed. Engl.* **1997**, *36*, 1085–1087. (b) Okuyama, M.; Ohkita, M.; Tsuji, T. *Chem. Commun.* **1997**, 1277–1278.

(8) (a) Tsuji, T.; Komiya, Z.; Nishida, S. *Tetrahedron Lett.* **1980**, *21*, 3583–3586. (b) Tsuji, T.; Nishida, S. *Tetrahedron Lett.* **1983**, *24*, 3361–3364.

Scheme 4



Scheme 5



Photochemical Behavior of the Dewar Benzene Precursors.

Reactivity common to the 1,4-C₄-bridged Dewar benzenes studied so far is clean, reversible photochemical transformation into the corresponding [4]paracyclophanes.³ Thus, as reported previously, irradiation of **30** with 254 nm light under matrix isolation at 77 K leads to the formation of **33** which cleanly reverts to **30** upon secondary irradiation with 365 nm light with which **33**, but not **30**, is electronically excited (Scheme 5).^{3a,b} Compounds **4**, **7**, **8**, **10**, **12**, **16**, and **17** photochemically behaved similarly, and their irradiation under matrix isolation at low temperature led to the development of new absorption bands at long wavelength regions, respectively, which rapidly decayed to restore the original spectra upon secondary irradiation with light of wavelengths selectively absorbed by the products, suggesting the transient generation of [4]paracyclophanes (Schemes 4 and 5). As described later, the photochemical generation of **24** from **8** and the ready reverse transformation upon secondary irradiation are indeed supported by ¹H NMR measurements.

Figure 1 shows difference UV-vis spectra between the absorptions before and after the irradiation of **7** with 254 nm light in ether-2-methylbutane glass at 77 K (spectra b and c) and that between those before and after the subsequent irradiation with light of wavelength >440 nm (spectrum d), together with the absorption spectrum for **7** (spectrum a). The difference spectrum d in Figure 1 unambiguously demonstrates the regeneration of **7** at the expense of the product generated in the prior irradiation with 254 nm light. These observations are best

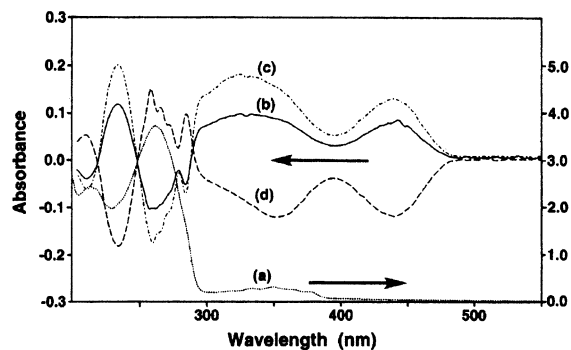


Figure 1. UV-vis absorption (a) and difference spectra (b-d) in ether-2-methylbutane (1:1) glass at 77 K: (a) for **7**;¹⁵ (b) (spectrum after irradiating 254 nm light for 30 s) minus (spectrum a); (c) (spectrum after irradiating 254 nm light for 1 min) minus (spectrum a); (d) (spectrum after subsequently irradiating >440 nm light for 1 min) minus (spectrum c).

accommodated by postulating the initial formation of **18**, and, accordingly, the characteristic absorption spectrum extending to 480 nm was assigned to **18**. The prepared Dewar benzenes are more or less prone to undergo irreversible photochemical transformation into the corresponding naphthalene derivatives. Thus, extended irradiation of matrix containing **7** led to the steady accumulation of **21** after the generation of **18** reached a plateau. The deviation of the difference spectrum d in Figure 1 from the mirror image of the spectrum c in the 300–340 nm region is primarily due to the formation of **21** during the irradiation of 254 nm light.¹⁶

Electronic absorption spectra for **4**, **10**, **12**, **16**, and **17** and difference spectra derived from their irradiation are shown in Figure 2. While the photochemical behavior of **4** and **10** is similar to that of **7**, compounds **8**, **16**, and **17** are less prone to isomerize to the naphthalene derivatives, and a photostationary state consisting of the Dewar benzene precursor and the corresponding [4]paracyclophane was reached after a short time of irradiation of each substrate. Dione **6** is at the other end of the reactivity spectrum and appeared to produce **20** almost exclusively upon irradiation under matrix isolation. Although the mechanism of the formation of the naphthalene derivatives is not clear at present, the exclusive formation of **20** from **6** suggests that they are derived from the triplet excited states of the Dewar benzene precursors, while the aromatization to the [4]paracyclophanes occurs in their singlet excited states. The photochemical reaction of **9** was complex, producing thermally labile products whose properties were consistent neither with the corresponding [4]paracyclophane **25** nor with the 1,4-naphthoquinone derivative **28**, and hence was not investigated further. The difference spectrum for **16**, that is, (c) in Figure 2D, is closely similar in shape to that reported for **33**,^{3a,b} except for the bathochromic shifts of absorption bands by 20–25 nm. The bending of the benzene ring leads to the rise of HOMO as well as the lowering of LUMO in energy.⁵ Parent [4]paracyclophane, as a result, exhibits absorption maxima in the 330–340 and 370–380 nm regions.^{3b} The observed spectra demonstrate that electronic interactions between those frontier molecular orbitals and the substituents give rise to the pronounced further bathochromic shifts of absorption bands.

(15) The weak absorption in the 300–380 nm region is due to the contaminant **8** (<2%).

(16) The formation of **21** was confirmed by ¹H NMR. See the Experimental Section.

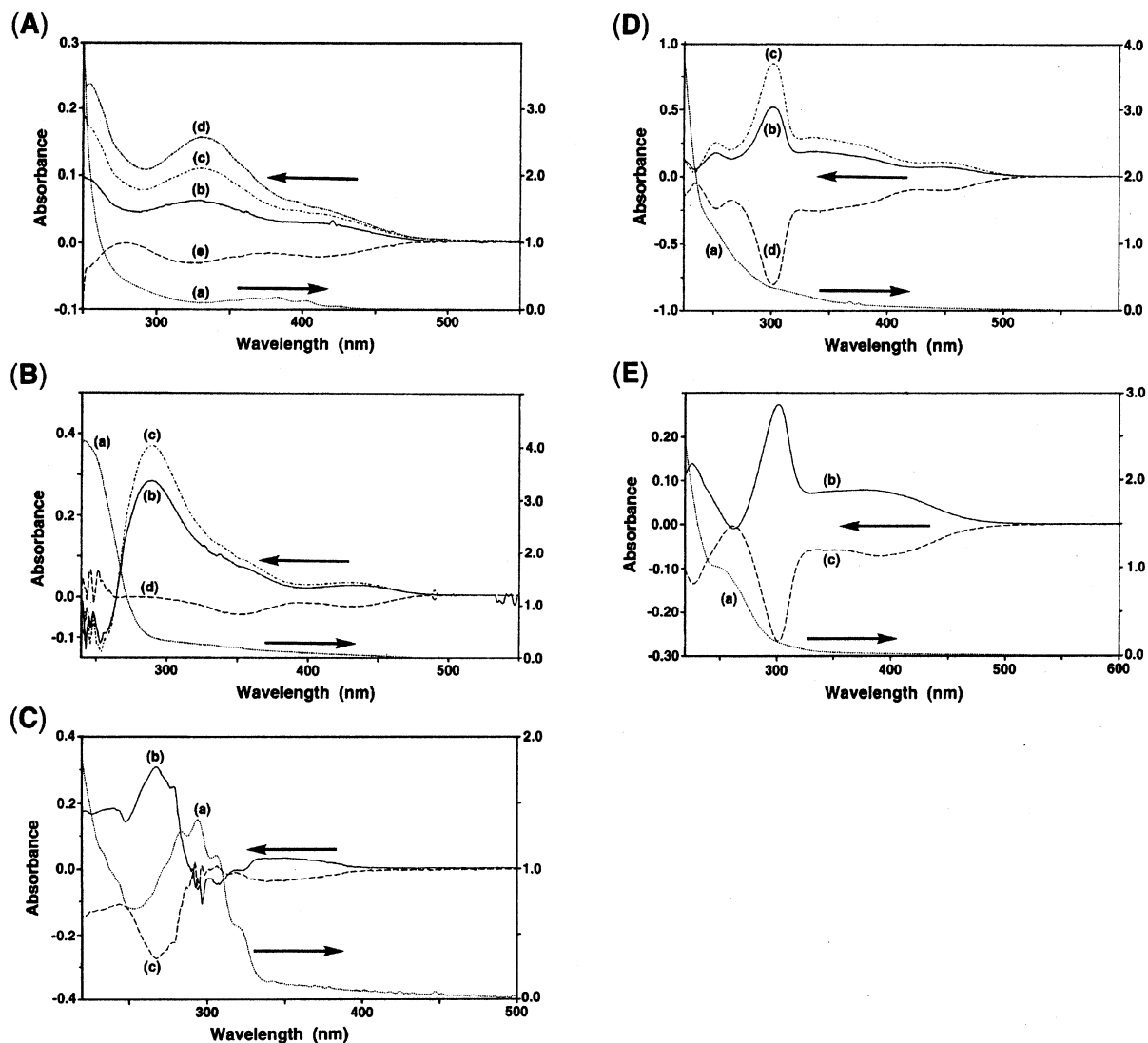


Figure 2. UV-vis absorption (a) and difference spectra (b–e) in ether–2-methylbutane (1:1) glass at 77 K. (A) (a) For **4**; (b) (spectrum after irradiating 254 nm light for 3 min) minus (spectrum a); (c) (spectrum after irradiating 254 nm light for 5 min) minus (spectrum a); (d) (spectrum after irradiating 254 nm light for 7 min) minus (spectrum a); (e) (spectrum after subsequently irradiating 365 nm light for 30 s) minus (spectrum d). (B) (a) For **10**; (b) (spectrum after irradiating 254 nm light for 10 s) minus (spectrum a); (c) (spectrum after subsequently irradiating 254 nm light for 20 s) minus (spectrum a); (d) (spectrum after subsequently irradiating >400 nm light for 30 s) minus (spectrum c). (C) (a) For **12**; (b) (spectrum after irradiating 313 nm light for 5 min) minus (spectrum a); (c) (spectrum after subsequently irradiating 365 nm light for 8 min) minus (spectrum b). (D) (a) For **16**; (b) (spectrum after irradiating 254 nm light for 1 min) minus (spectrum a); (c) (spectrum after irradiating 254 nm light for 3 min) minus (spectrum a); (d) (spectrum after subsequently irradiating >470 nm light for 5 min) minus (spectrum c). (E) (a) For **17**; (b) (spectrum after irradiating 254 nm light for 5 min) minus (spectrum a); (c) (spectrum after subsequently irradiating >440 nm light for 6 min) minus (spectrum b).

Kinetic Stabilities of [4]Paracyclophanes. [4]Paracyclophane, for example, **33**, remains unchanged indefinitely under matrix isolation at 77 K but is highly labile in fluid solution, polymerizing almost instantaneously even at $-130\text{ }^{\circ}\text{C}$,³ unless some stabilizing measures are undertaken. The lability of [4]-paracyclophane undoubtedly arises from its susceptibility at the bridgehead carbon atoms toward the addition of diverse reagents, by which means steric strain inherent to the structure is largely relieved. [4]Paracyclophanes preferentially react indeed with trapping reagents at their bridgehead carbon atoms.^{2,3} This implies that the ring system may be kinetically stabilized by introducing sterically demanding substituents which serve to sterically hinder reactions at the reactive bridgehead sites. The [4]paracyclophane derivatives herein studied were designed on the basis of such consideration.

Glass matrixes containing the [4]paracyclophanes were thawed, and their kinetic stabilities were evaluated by monitoring

Table 1. Kinetic Stabilities of the Substituted [4]Paracyclophanes in Ether–2-Methylbutane (1:1)

compd	temp (°C)	$t_{1/2}$ (min)	content (%) ^a	compd	temp (°C)	$t_{1/2}$ (min)	content (%) ^a
18	-90	10 ± 3	$\leq 6^b$	29	-50	30 ± 5	$\leq 2^d$
19	-20	30 ± 5	$\leq 3^b$	31	-130	20 ± 5	$\leq 15^b$
24	-20	12 ± 2	$\leq 10^c$	32	-50	100 ± 10	$\leq 5^b$

^a At a quasi-photostationary state reached upon irradiation of the corresponding Dewar benzene isomer. ^b Under irradiation of 254 nm light. ^c Under irradiation of 365 nm light. ^d Under irradiation of 313 nm light.

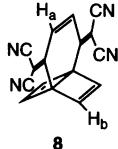
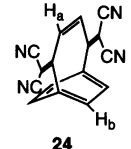
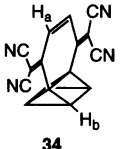
their decay spectrometrically. The results summarized in Table 1 show that significant improvement in kinetic stability has been achieved in **19**, **24**, **29**, and **32**. The stabilities of **19** and **24** are, while comparable to each other, much superior to those of the other [4]paracyclophanes examined. Cyclophane **18** is much less stable than **24** rather unexpectedly and disappears fairly rapidly even at $-90\text{ }^{\circ}\text{C}$. Although the cause of the poor stability of **18**

is not entirely clear, examination of molecular models of **18** and **24** is revealing. While the geometry-optimized structure of **24** is C_{2v} symmetric (vide infra) and the cyano substituents effectively hinder destructive reactions at the bridgehead positions, the $-\text{CH}_2\text{CH}_2-$ moiety of **18** preferentially adopts a staggered conformation as is the case with parent [4]paracyclophane,^{4–6} thereby displacing the dicyanomethylene groups from the plane bisecting the bent aromatic ring and, thus, making the access to the bridgehead carbon atoms less sterically encumbered. The stabilities of **29** and **32** are only intermediate among the derivatives investigated, because of the conformational flexibility which allows the substituents to deviate from the desired, bridgehead-protecting arrangements.

¹H NMR Spectrum of 24. The measurement of the ¹H NMR spectrum of [4]paracyclophane ought to provide not only definitive evidence for its formation but also valuable information concerning the aromaticity of its severely bent benzene ring, but has been thwarted because of the extreme thermal instability. The improved thermal stability of **24**, however, is high enough to permit the measurement of the ¹H NMR spectrum. Another requisite to be fulfilled to measure an NMR spectrum of [4]paracyclophane is its content at the quasi-photostationary state reached upon irradiation of the Dewar benzene precursor. Fortunately, the proportion of **24** to **8** at the quasi-photoequilibrium under irradiation of 365 nm light was sufficiently high as listed in Table 1.

The ¹H NMR spectrum of **8** consists of a pair of singlets at δ 6.93 and 7.20 in an intensity ratio of 2:1 in CD_2Cl_2 . Irradiation of **8** with 365 nm light at -90°C led to the development of a pair of weak singlet signals with an intensity ratio of ca. 2:1 at δ 7.97 and 5.85, which rapidly decayed upon subsequent irradiation with light of wavelength >400 nm to restore the original two line spectrum.^{7a} The observed photochemical behavior of the transient and its simple ¹H NMR spectrum are consistent with the formation of **24**. Corroborating evidence for this assignment was provided by the theoretical calculations of proton chemical shifts.¹⁷ Thus, the calculations for **8** and **24** using the gauge-independent atomic orbital (GIAO) method¹⁸ at the hybrid HF-DFT (B3LYP/6-31+G*) level of theory satisfactorily reproduce the experimental spectra as summarized in Chart 1. The experimental and computed chemical shift changes ($\Delta\delta$) accompanying the rearrangement of **8** to **24** agree particularly well with each other. Prismane derivative **34** is apparently incompatible with the observed spectrum. The pronounced upfield shift of H_a signal ($\Delta\delta = -1.35$ ppm) accompanied by the marked downfield shift of H_b ($\Delta\delta = 1.04$ ppm) upon the isomerization of **8** to **24** strongly suggests the sustenance of a substantial diamagnetic ring current in the

Chart 1. Experimental and Calculated (in Parentheses, GIAO/B3LYP/6-31+G*) Proton Chemical Shifts for **8**, **24**, and **34**, and Chemical Shift Changes ($\Delta\delta$) Accompanying Rearrangement of **8** to **24** and **34**

			
	8	24	34
$\delta(H_a)$	7.20 (6.96)	5.85, $\Delta\delta = -1.35$ (5.59, $\Delta\delta = -1.37$)	— (7.28, $\Delta\delta = 0.08$)
$\delta(H_b)$	6.93 (6.73)	7.97, $\Delta\delta = 1.04$ (7.84, $\Delta\delta = 1.11$)	— (4.03, $\Delta\delta = -2.70$)

benzene ring of the latter despite its extreme bending. The exhibition of significant diatropicity by such a severely bent benzene ring was rather unexpected^{6,19} and seemed to deserve further investigation. In the following section, the aromaticity of **24** was investigated theoretically. The calculations of chemical shifts for **8** and **24** at the RHF/6-31G* and RHF/6-31+G* levels were less satisfactory, for example, providing δ 7.19 and 7.02 and δ 5.52 ($\Delta\delta = -1.67$) and 8.50 ($\Delta\delta = 1.48$) for the H_a and H_b of **8** and **24**, respectively, at the latter level. The theoretical examination on **24** described below is, therefore, based on the calculations at the B3LYP/6-31+G* level unless otherwise noted.

Aromaticity of the Extremely Bent Benzene Moiety of 24.

The principal geometrical parameters for geometry-optimized **24** are summarized in Table 2. The structure of **24** is C_{2v} symmetric,²⁰ and the planar bis(dicyanomethylene)buteno bridge bisects the bent benzene ring. The deformation angles α and β , which give a measure of the degree to which the benzene ring is bent, are 28.6° and 43.9° , respectively, and the sum ($\alpha + \beta$) amounts to 72.5° . As a result, the bridgehead carbon atoms are markedly pyramidalized, decreasing the sum of the bond angles around each of them to 341.5° from 360° for a planar trivalent carbon atom. The residual aromatic carbon atoms are also pyramidalized (the sum of the bond angles is 356.0°) as illustrated in Table 2, so as better to maintain π -orbital overlap with the adjacent bridgehead carbon atom.²¹

A number of definitions or criteria have been considered for characterizing aromaticity.²² The majority are, however, applicable only for nearly planar aromatic compounds and often disturbed by strain effects and other contributing factors. Schleyer and co-workers recently proposed two probes, the diamagnetic susceptibility exaltation (Λ)²³ and the nucleus-

(17) All calculations were performed with the programs implemented in the Gaussian 98 program package. Frisch, M. J.; Trucks, G. W.; Schlegel, H. B.; Scuseria, G. E.; Robb, M. A.; Cheeseman, J. R.; Zakrzewski, V. G.; Montgomery, J. A., Jr.; Stratmann, R. E.; Burant, J. C.; Dapprich, S.; Millam, J. M.; Daniels, A. D.; Kudin, K. N.; Strain, M. C.; Farkas, O.; Tomasi, J.; Barone, V.; Cossi, M.; Cammi, M.; Mennucci, B.; Pomelli, C.; Adamo, C.; Clifford, S.; Ochterski, J.; Petersson, G. A.; Ayala, P. Y.; Cui, Q.; Morokuma, K.; Salvador, P.; Dannenberg, J. J.; Malick, D. K.; Rabuck, A. D.; Raghavachari, K.; Foresman, J. B.; Cioslowski, J.; Ortiz, J. V.; Baboul, A. G.; Stefanov, B. B.; Liu, G.; Liashenko, A.; Piskorz, P.; Komaromi, I.; Gomperts, R.; Martin, R. L.; Fox, D. J.; Keith, T.; Al-Laham, M. A.; Peng, C. Y.; Nanayakkara, A.; Challacombe, M.; Gill, P. M. W.; Johnson, B.; Chen, W.; Wong, M. W.; Andres, J. L.; Gonzalez, C.; Head-Gordon, M.; Replogle, E. S.; Pople, J. A. *Gaussian 98*, revision A.11.1; Gaussian, Inc.: Pittsburgh, PA, 2001.

(18) Wollinski, K.; Hinton, J. F.; Pulay, P. *J. Am. Chem. Soc.* **1990**, *112*, 8251–8260.

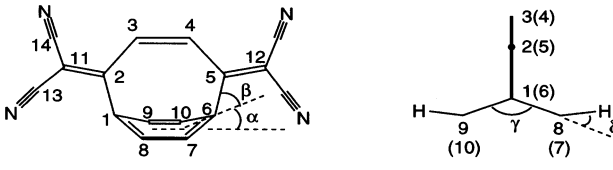
(19) For the diatropicity of [5]paracyclophanes which bear less strained benzene rings than [4]paracyclophane, see: (a) Jenneskens, L. W.; de Kanter, F. J. J.; Kraakman, P. A.; Turkenburg, L. A. M.; Koolhaas, W. E.; de Wolf, W. H.; Bickelhaupt, F.; Tobe, Y.; Kakiuchi, K.; Odaira, Y. *J. Am. Chem. Soc.* **1985**, *107*, 3716–3717. (b) Tobe, Y.; Kaneda, T.; Kakiuchi, K.; Odaira, Y. *Chem. Lett.* **1985**, 1301–1304. (c) Kostermans, G. B. M.; de Wolf, W. H.; Bickelhaupt, F. *Tetrahedron Lett.* **1985**, *27*, 1095–1098. (d) Kostermans, G. B. M.; de Wolf, W. H.; Bickelhaupt, F. *Tetrahedron* **1987**, *43*, 2955–2966.

(20) The geometry optimizations of **24** starting from the various less symmetrical geometries converged to the C_{2v} symmetric one.

(21) Haddon, R. C. *Acc. Chem. Res.* **1988**, *21*, 243–249 and references therein.

(22) (a) Garrat, P. J. *Aromaticity*; Wiley & Sons: New York, 1986. (b) Minkin, V. I.; Glukhovtsev, M. N.; Simkin, B. Y. *Aromaticity and Antiaromaticity: Electronic and Structural Aspects*; Wiley & Sons: New York, 1994.

(23) Schleyer, P. v. R.; Jiao, H. *Pure Appl. Chem.* **1996**, *68*, 209–218. This criterion was first proposed by Dauben et al.: Dauben, H. J., Jr.; Wilson, J. D.; Laity, J. L. *J. Am. Chem. Soc.* **1968**, *90*, 811. Dauben, H. J., Jr.; Wilson, J. D.; Laity, J. L. *J. Am. Chem. Soc.* **1969**, *91*, 1991.

Table 2. Selected Geometrical Parameters for C_{2v} Symmetric **24** Optimized at the B3LYP/6-31+G* Level of Theory


Bond Lengths and Nonbonding Interatomic Distances (Å)			
C1–C2	1.4993	C11–C14	1.4340
C2–C3	1.4859	C13–N	1.1639
C3–C4	1.3868	C14–N	1.1638
C1–C8	1.4122	C3–H	1.0892
C7–C8	1.3921	C7–H	1.0876
C2–C11	1.3784	C1...C6	2.6756
C11–C13	1.4325	C7...C10	2.4165

Bond, Torsional, and Bending Angles (deg)			
C1–C2–C3	114.944	C1–C8–H	120.429
C1–C2–C11	124.595	C7–C8–H	118.518
C1–C8–C7	117.030	C1–C8–C7–H	157.565
C2–C3–C4	137.527	C3–C2–C1–C8	67.253
C3–C2–C11	120.461	C7–C8–C1–C2	–99.164
C2–C1–C8	111.908	C7–C8–C1–C9	32.503
C8–C1–C9	117.657	α	28.597
C2–C11–C13	120.477	β	43.874
C2–C11–C14	123.358	γ	147.703
C2–C3–H	111.244	δ	22.435

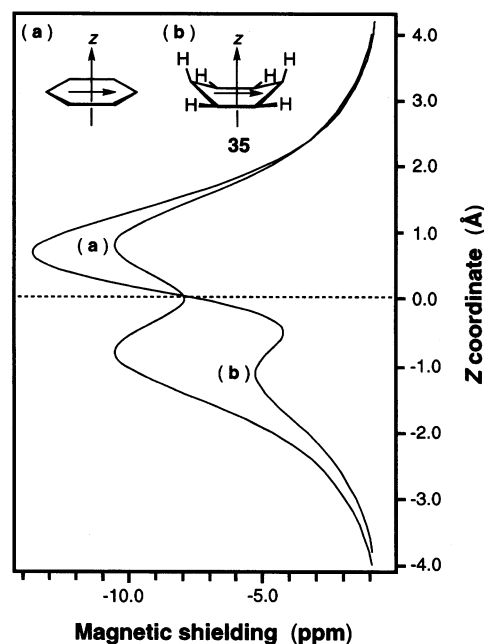
independent chemical shift (NICS),²⁴ as effective aromaticity/antiaromaticity criteria, applicable not only for planar molecules but also for nonplanar ones including spherical systems. According to these definitions, significantly exalted (negative) Λ and negative NICS denote aromaticity, whereas positive Λ and NICS indicate antiaromaticity. NICS value calculated at the center (mean of the carbon atom coordinates) of the C_6 ring moiety of **24** is -8.1 (GIAO/B3LYP/6-31+G*) as compared with -9.7 for planar benzene, and Λ computed for the bent benzene **35**²⁵ whose geometry was constrained to that present in **24** is -11.5 ppm cgs²⁶ (CSGT/B3LYP/6-311+G**) as compared with -15.1 ppm cgs for planar benzene,²⁸ suggesting that aromaticity is retained to a considerable extent in **24**. NICS value at the center of **35** is -7.7 , and the chemical shift for the protons on the edge carbon atoms is δ 7.92,³⁰ in good agreement with those calculated for **24**. Thus, **35** seems to be an adequate model for the examination of the aromaticity of **24**. Schaefer and co-workers have shown that the boat-shaped benzene with the same geometry as that in [4]paracyclophane has almost the same magnetic susceptibility as the hypothetical cyclohexatriene with alternating single and double bonds (Table 3), and, therefore, a weak ring current is expected in [4]paracyclophane.⁶ The magnetic susceptibility data for **35** computed using the

- (24) Schleyer, P. v. R.; Maerker, C.; Dransfeld, A.; Jiao, H.; van Eikema Hommes, N. J. R. *J. Am. Chem. Soc.* **1996**, *118*, 6317–6318.
 (25) The benzene ring was frozen in the conformation present in **24**, two hydrogen atoms were placed in the same direction as the benzylic carbon atoms, and the C–H bond lengths were optimized at the B3LYP/6-31+G* level.
 (26) Calculated using the increment system derived from the computed magnetic susceptibility data for ethylene and 1,3-butadiene. For derivation of Λ , see refs 27 and 28.
 (27) Fleischer, U.; Kutzelnigg, W.; Lazzarotti, P.; Mühlenkamp, V. *J. Am. Chem. Soc.* **1994**, *116*, 5298–5306.
 (28) Simion, D. V.; Sorensen, T. S. *J. Am. Chem. Soc.* **1996**, *118*, 7345–7352.
 (29) Continuous set of gauge transformations method: (a) Keith, T. A.; Bader, R. F. W. *Chem. Phys. Lett.* **1992**, *194*, 1–8. Keith, T. A.; Bader, R. F. W. *Chem. Phys. Lett.* **1993**, *210*, 223–231. (b) Cheeseman, J. R.; Frisch, M. J.; Trucks, G. W.; Keith, T. A. *J. Chem. Phys.* **1996**, *104*, 5497–5509.
 (30) Calculated chemical shift for the protons at the bow and stern positions of **35** is δ 5.85.

Table 3. Magnetic Susceptibility Data (ppm cgs with Sign Reversed)^a

compd	IGLO/TZP				CSGT/B3LYP/6-311+G**			
	χ_{ip}	χ_{zz}	χ_{av}	$\Delta\chi$	χ_{ip}	χ_{zz}	χ_{av}	$\Delta\chi$
benzene ^{b,c}	46.8	110.2	68.0	63.4	30.4	97.9	52.9	67.5
bent benzene ^d	45.0	100.5	63.5	55.5				
35					30.6	86.6	49.3	56.0
hypothetical cyclohexatriene ^e	46.1	100.6	64.2	54.6	30.8	93.2	51.6	62.4

^a χ_{ip} is the in-plane component: $\chi_{ip} = (\chi_{xx} + \chi_{yy})/2$. χ_{zz} is the out-of-plane component. χ_{av} is the isotropic part: $\chi_{av} = (2\chi_{ip} + \chi_{zz})/3$. $\Delta\chi$ is the anisotropic part: $\Delta\chi = \chi_{zz} - \chi_{ip}$. ^b IGLO/TZP: ref 27. CSGT/B3LYP/6-311+G**: ref 28. ^c Experimental values: $\chi_{ip} = 34.9 \pm 2.0$, $\chi_{zz} = 94.6 \pm 2.5$, $\chi_{av} = 54.8$, and $\Delta\chi = 59.7$ ppm cgs (with sign reversed): ref 31. ^d With the same geometry as in the DZ+d SCF optimized [4]paracyclophane: ref 6. ^e With alternating single and double bonds: $r(C-C) = 1.501$ Å, $r(C=C) = 1.336$ Å, $r(C-H) = 1.083$ Å, and all angles equal to 120° . IGLO/TZP: ref 27. CSGT/B3LYP/6-311+G**: this work.

**Figure 3.** Plots of calculated magnetic shielding effect in ppm (GIAO/B3LYP/6-31+G*) versus distance from the ring center along the z axis for (a) planar benzene and (b) the bent benzene **35** with the same geometry as that in **24**. Negative shielding denotes diamagnetic effect.

CSGT/B3LYP/6-311+G** are listed in Table 3, together with those for the hypothetical cyclohexatriene.

In Figure 3 are illustrated plots of absolute magnetic shieldings (NICS) computed for planar benzene and **35** along their z axes. The maximum diamagnetic shieldings found above and below the ring center of benzene reflect the π electron toroid density.²⁴ The magnitude of diamagnetic shielding effect in **35** is markedly unsymmetrical with respect to the plane of bent benzene ring, and the effect in the region of space above the concave surface is significantly stronger than that below the convex surface. As described above, all of the carbon atoms of the boat-shaped **35** are extensively pyramidalized so as better to maintain the π -orbital overlaps, and the axes of the atomic π -orbitals, those at the bow and stern in particular, are tilted toward the concave side. The π -orbitals may, as a result, overlap with each other more effectively above the concave surface than below the convex surface, and the diamagnetic ring current induced above the former may consequently be stronger than that below the latter. It should also be noted that the diamag-

netically shielded region of space above the concave surface seems to be restricted to concentrate the effect within a relatively narrow space along the z coordinate because of the tilting of the atomic π -orbitals, as compared to that below the reverse surface which appears to be extended to the wider space. The stronger diamagnetic shielding effect above the concave surface may, partially at least, be due to reinforcement by the local shielding effect by the tilted π -orbitals at the bow and stern of **35**. The magnitude of this local effect may be estimated by calculating magnetic shielding for 1,3-butadiene, whose geometry is constrained to that of the C3–C2–C1–C6 moiety of **35**.³² The results suggest that the diamagnetic shielding in the concave region 0.6–2.0 Å above the ring center of **35** is enhanced by this local effect, but the enhancement will be less than 3 ppm. Because the magnetic shielding effect calculated for nonconjugated, planar 1,4-cyclohexadiene along the z axis decays monotonically with increasing distance from the ring center, the appearance of maxima in magnetic shielding above and below the bent benzene ring of **35** is also consistent with the maintenance of the aromatic conjugation. Thus, **35** and, accordingly, **24** seem to sustain substantial aromaticity despite the extreme bending of their C₆ rings, as judged by the magnetic criteria of aromaticity, Λ and NICS.

The aromatic stabilization energy of benzene has been evaluated at 25 ± 5 kcal mol⁻¹,²² while the energy difference between planar benzene and **35** is 87 kcal mol⁻¹ at the B3LYP/6-31+G* level. The aromatic stabilization energy of **35** thus compensates only a fraction of its strain energy at best. In benzene, distortion into a nonplanar geometry unavoidably gives rise to the torsion of π -bonds, which is not suppressible by the localization of π -bonds. Thus, the carbon atoms of benzene undergo extensive rehybridization-pyramidalization upon severe bending to avoid the rupture of π -bonds leading to degeneration into a biradical(oid), at the expense of energy even much greater than its aromatic stabilization energy, and, consequently, the cyclic conjugation seems to be retained. The sustenance of aromatic conjugation in **24** is, thus, basically not attributable to the aromatic stabilization effect. Accordingly, the benzene ring moiety of **24** is extremely bent and strained, yet it sustains rather strong diatropicity and only a small degree of bond alternation.

Thermal Cycloreversion of 24 to 8. The investigation of the thermal behavior of **24** revealed that its insufficient stability for isolation at ambient temperature was due to the reactivity to undergo spontaneous reversion to **8** below 0 °C rather than the insufficient protection of its reactive bridgehead sites toward intermolecular reactions. The difference UV–vis spectrum between the spectra taken before and after a cycle of thawing an ether–2-methylbutane matrix containing **24**—brief warming to room temperature—refreezing at 77 K clearly displayed the regeneration of **8** at the expense of **24** (Figure 4). This observation indicates that **24** is higher in energy than **8** and thermally reverts to the latter rapidly at room temperature. The measured half-life of **24** is 15 ± 5 min at –20 °C, and, accordingly, the activation free energy for the isomerization of **24** to **8** is 18.3 ± 0.3 kcal mol⁻¹. The calculated energy of **8**

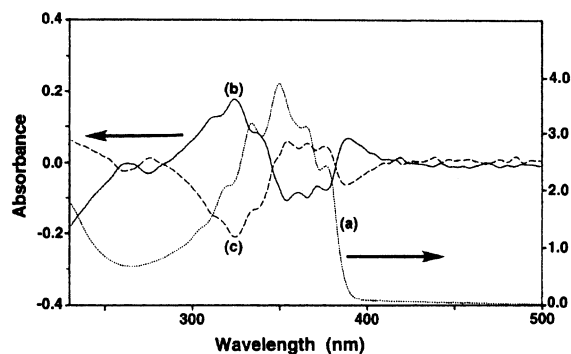


Figure 4. UV–vis absorption (a) and difference spectra, (b) and (c), in ether–2-methylbutane (1:1) glass at 77 K: (a) for **8**; (b) (spectrum after irradiating 365 nm light for 7 min) minus (spectrum a); (c) (spectrum after briefly heating the resulting mixture to ambient temperature in the dark) minus (spectrum b).

relative to **24** is -20.3 kcal mol⁻¹ at the B3LYP/6-31+G* level, supporting the substantial exothermicity of the isomerization process. The agreement of this energy barrier with a value of 22 kcal mol⁻¹ computed for the rearrangement of parent [4]-paracyclophane to the Dewar benzene isomer⁶ is extremely good, especially when a higher exothermicity for the process from **24** to **8** is taken into account.

Steric strain in paracyclophane is rapidly accumulated as a bridging side chain is shortened, whereas the strain in the corresponding Dewar benzene form remains largely unaffected.^{4,5} Thus, it is expected that the thermodynamic stability order, benzene form > Dewar form, is reversed at a certain chain length and the former becomes more energetic than the latter. This reversion of the stability order has been predicted by theoretical calculations for a pair of [4]paracyclophane/1,4-(CH₂)₄-bridged Dewar benzene,⁶ but it remained experimentally unverified because of the extreme instability of [4]paracyclophane. The thermal rearrangement of **24** to **8** represents the first experimental verification of the theoretical prediction. Thus, the kinetic stability of the [4]paracyclophane system is defined not only by the susceptibility of its bridgehead carbon atoms toward the addition of diverse reagents, but also by the intrinsic thermal reactivity to rearrange to the Dewar form. Further shortening of the side chain will certainly result in a lowered energy barrier to isomerization to the Dewar form and hence in a reduced lifetime of the benzene form. Compound **24** seems to represent almost a limiting case of experimentally characterizable strained paracyclophanes.

Conclusion

Irradiation of 1,4-bridged Dewar benzenes bearing a variety of functional groups led more or less successfully to the formation of the corresponding [4]paracyclophanes, which underwent efficient cycloreversion upon subsequent electronic excitation. [4]Paracyclophane is a highly labile species, but could be stabilized kinetically by introducing substituents which sterically hinder access to the reactive bridgehead carbon atoms by other reagents to an extent to allow the measurement of the ¹H NMR spectrum. The recorded spectrum suggested that the [4]paracyclophane derivative sustains significant diatropicity despite the extreme bending of its benzene ring. Theoretical calculations also support the retention of substantial aromaticity in the bent benzene moiety as judged by the magnetic criteria of aromaticity, that is, diamagnetic susceptibility exaltation and

(31) (a) Hoarau, J.; Lumbroso, N.; Pacult, N. *C. R. Acad. Sci.* **1956**, *242*, 1702. (b) Flygare, W. H. *Chem. Rev.* **1974**, *74*, 653–687.

(32) Under the constraint of all of the bond and dihedral angles to the corresponding angles in the C3–C2–C1–C6 moiety of **35**, all of the bond lengths were optimized. The magnitude of magnetic shielding in the region of space corresponding to 0.6–2.0 Å above the ring center of **35** is -0.6 to -1.5 ppm.

NICS. [4]Paracyclophane is so strained that the [4]paracyclophane derivative **24** exceeds the corresponding Dewar benzene form **8** in energy and undergoes thermal cycloreversion to **8** with a half-life of 15 ± 5 min at -20 °C ($\Delta G^\ddagger = 18.3 \pm 0.3$ kcal mol⁻¹). Thus, the kinetic stability of [4]paracyclophane is defined not only by the propensity to undergo destructive intermolecular reactions at the bridgehead sites, but also by the intrinsic thermal reactivity to rearrange to the Dewar benzene form.

Experimental Section

General. ¹H and ¹³C NMR spectra were recorded on a JEOL EX-400 (¹H/400 MHz, ¹³C/100 MHz) spectrometer in CDCl₃ unless otherwise indicated. IR spectra were taken on a Hitachi Model 215 grating spectrometer. Mass spectra were recorded on JEOL JMS-DX 300 (EI) and JMS-01SG-2 (FD) spectrometers. UV-vis spectra were taken on a Hitachi U-4000 spectrophotometer. Column and thin-layer chromatography (TLC) were performed on silica gel 60 (Merck) of particle size 63–200 and 5–20 μm, respectively. HPLC was carried out on LiChrosorb Si60 (Merck, 7 μm). Elemental analyses were performed by the Center for Instrumental Analysis of Hokkaido University. Halos (Eiko-sha, Japan) 450 W high-pressure and 120 W low-pressure mercury lamps were employed as the light sources of photochemistry. A 450 W high-pressure mercury lamp fitted with a jacket containing an aqueous K₂CrO₄ solution and a Corning 7-54 glass filter, that with a Corning 0-52 filter, and that with Corning 0-52 and 7-60 filters were used as 313, >340, and 365 nm light sources, respectively. A 500 W xenon lamp fitted with a Corning 3-71 glass filter, that with a Corning 3-72 filter, and that with a Corning 3-73 filter were used as >470, >440, and >400 nm light sources, respectively. Tricyclo[4.2.2.0^{1,6}]deca-2,4,7,9-tetraene,^{3d} 1,4-bis(trimethylsilyl)-2-butyne,³³ and 4,5,6,7-tetrahydro-1-indanone were prepared following the known procedures. Other reagents and solvents were obtained from commercial sources and purified prior to use.

Preparation of **2 from **1**.** A solution of 103 mg of **1** (0.80 mmol) and 5 mg of 5,10,15,20-tetraphenyl-21*H*,23*H*-porphine (TPP, 8 μmol) in 36 mL of CCl₄ was irradiated under gentle bubbling of O₂ with a 500 W Xe lamp fitted with a Corning 3-73 filter at 0 °C for 5 h. The resulting mixture was concentrated in vacuo and subjected to chromatography on silica gel eluted with CH₂Cl₂–hexane (1:1) to afford 123 mg of **2** (95%) as colorless crystals. ¹H NMR: δ 5.10–5.17 (m, AA' part of AA'XX', 2H), 6.30–6.38 (s at δ 6.34 and XX' part of AA'XX', 4H), 6.87 (s, 2H). ¹³C NMR: δ 52.78, 78.31, 126.81, 142.70, 144.15. IR (KBr): 3052, 2948, 1365, 1285, 1252, 1140, 1057, 962, 935, 900, 810, 780, 752, 717, 700 cm⁻¹. EI-MS: *m/z* 160 (M, 0.42), 128 (100), 102 (45), 77 (26), 51 (41). EI-HRMS for C₁₀H₈O₂: calcd 160.0525, found 160.0518.

Conversion of **2 to **3**.** To a solution of **2** (39 mg, 0.24 mmol) in 3 mL of CH₂Cl₂ was added Et₃N (61 mg, 0.60 mmol) under argon at 0 °C. After being stirred 2 h at 0 °C and then 12 h at 5 °C, the resulting mixture was concentrated and subjected to chromatography on silica gel eluted with ether to produce 37 mg of **3** (95%) as a colorless oil. ¹H NMR: δ 1.94 (d, *J* = 8.4 Hz, 1H), 4.90 (br d, *J* = 8.4 Hz, 1H), 5.86 (dd, *J* = 10.2, 2.3 Hz, 1H), 6.52–6.77 (m, 5H). ¹³C NMR: δ 61.58, 65.82, 66.51, 126.57, 140.12, 141.26, 143.78, 144.13, 147.57, 197.29. IR (neat): 3600–3200 (br), 1674, 1380, 1302, 1214, 1086, 1064, 844, 794, 738 cm⁻¹. EI-MS: *m/z* 160 (M, 0.33), 131 (20), 115 (100), 104 (31), 77 (47), 51 (31). EI-HRMS for C₁₀H₈O₂: calcd 160.0525, found 160.0501. UV λ_{max} (ether): 203 (sh, ε 9000), 335.0 (39), 345.5 (39) nm.

Oxidation of **3 to **4**.** To a solution of 13 mg of **3** (81 μmol) in 2 mL of CH₂Cl₂ was added 85 mg of MnO₂. After being stirred 2 h at room

temperature, the resulting mixture was filtered and subjected to chromatography on silica gel eluted with ether–hexane (1:1) to afford 12 mg of **4** (92%) as pale yellow crystals. ¹H NMR: δ 6.59 (s, 2H), 6.70 (s, 4H). ¹³C NMR: δ 65.91, 140.09, 140.38, 195.21. IR (KBr): 3064, 1676, 1658, 1592, 1300, 1100, 1014, 808, 752 cm⁻¹. EI-MS: *m/z* 158 (M, 2), 130 (25), 104 (70), 102 (80), 76 (100), 50 (51). EI-HRMS for C₁₀H₈O₂: calcd 158.0368, found 158.0365. UV-vis λ_{max} (ether): 229 (ε 14 000), 367 (113), 380 (113), 400 (sh, 75), 423 (sh, 19) nm.

Reduction of **3 to **5**.** To a solution of 87 mg of **3** (0.54 mmol) and 19 mg of Pd(PPh₃)₄ (16 μmol) in 29 mL of THF was added 177 mg of Bu₃SnH (0.61 mmol) under argon at 0 °C. After being stirred 0.5 h, the mixture was concentrated and subjected to chromatography on silica gel eluted with ether to afford 74 mg of **5** (84%) as a colorless oil. ¹H NMR: δ 1.78 (br s, 1H), 1.9–2.1 (m, 2H), 2.3–2.6 (m, 2H), 4.43 (t, *J* = 4.5 Hz, 1H), 6.55–6.75 (m, 4H). ¹³C NMR: δ 28.97, 36.54, 65.20, 66.61, 68.22, 140.22, 141.35, 142.03, 144.42, 208.45. IR (neat): 3450 (br), 1705, 1295, 1220, 1110, 1075, 918, 800, 749 cm⁻¹. EI-MS: *m/z* 162 (M, 0.4), 131 (17), 115 (100), 104 (25), 77 (54), 51 (37). FD-HRMS for C₁₀H₁₀O₂: calcd 162.0681, found 162.0690.

Oxidation of **5 to **6**.** To a solution of 74 mg of **5** (0.46 mmol) in 2 mL of CH₂Cl₂ was added 148 mg of PCC (0.69 mmol) at 0 °C. After being stirred 3 h at room temperature, the mixture was filtered through a short column of Florisil, and the filtrate was subjected to chromatography on silica gel eluted with ether–hexane (1:2) to afford 65 mg of **6** (89%) as a colorless oil. ¹H NMR: δ 2.76 (s, 4H), 6.69 (s, 4H). ¹³C NMR: δ 37.80, 68.60, 140.71, 204.21. IR (neat): 1702, 1424, 1300, 1278, 1134, 800 cm⁻¹. EI-MS: *m/z* 160 (M, 0.97), 104 (98), 76 (100), 50 (54). FD-HRMS for C₁₀H₈O₂: calcd 160.0525, found 160.0528.

Condensation of Malononitrile to **6.** To a mixture of 23 mg of **6** (0.14 mmol) and 135 mg of malononitrile (2.0 mmol) was added a solution of 0.75 mg of β-alanine (8.4 μmol) in 0.15 mL of water. After being stirred 90 h at room temperature, the resulting mixture was diluted with 10 mL of CH₂Cl₂, washed with 5% Na₂CO₃ (×5) and brine, dried (MgSO₄), and concentrated to give 31 mg of crude product, which was crystallized from CH₂Cl₂–hexane to afford 22 mg of **7** (61%) as colorless crystals. ¹H NMR: δ 2.97 (s, 4H), 6.94 (s, 4H). IR (KBr): 2232, 1600, 1592, 1424, 1252, 784, 734, 560 cm⁻¹. FD-MS: *m/z* 257 (M + 1, 20), 256 (M, 100). FD-HRMS for C₁₆H₈N₄: calcd 256.0749, found 256.0733; UV λ_{max} (ether): 219 (sh, ε 11 000), 258 (28 000) nm. Compound **7** is susceptible to oxidation to produce **8**, and the samples of **7** thus prepared were invariably contaminated by a small amount of **8**.

Conversion of **7 to **8**.** To a solution of 22 mg of **7** (87 μmol) in 0.6 mL of CH₃CN were added 30 mg of pyridinium bromide perbromide (94 μmol) and, after 10 min, 15 mg of pyridine (0.19 mmol) under argon at 0 °C. After being stirred 1.5 h at 0 °C, the mixture was diluted with 20 mL of ether, washed with 1 N HCl (×3), water, and brine, dried (MgSO₄), and filtered through a short column of neutral alumina. The filtrate was concentrated, and the residue was crystallized from CH₂Cl₂–hexane to afford 16 mg of **8** (73%) as colorless crystals. ¹H NMR: δ 6.90 (s, 4H), 7.14 (s, 2H). ¹³C NMR: δ 162.36, 142.92, 131.35, 111.43, 110.11, 89.16, 58.03. IR (KBr): 2228, 1556, 806, 758, 526 cm⁻¹. FD-MS: *m/z* 255 (M + 1, 20), 254 (M, 100). FD-HRMS for C₁₆H₈N₄: calcd 254.0592, found 254.0603. UV λ_{max} (ether): 314 (sh, ε 66 000), 332 (110 000), 346 (140 000), 361 (110 000) nm.

Condensation of *t*-Butyl Malonate to **6.** To 2.1 mL of dry THF were added a solution of 351 mg of TiCl₄ (1.86 mmol) in 0.21 mL of CCl₄ and, after 15 min at 0 °C, a solution of 17 mg of **6** (0.11 mmol), 220 mg of *tert*-butyl malonate (1.02 mmol), and 632 mg of pyridine (7.99 mmol) in 1.04 mL of THF. After being stirred 32 h at room temperature, the resulting mixture was diluted with 30 mL of ether, filtered, and concentrated in vacuo to remove pyridine and the unreacted *tert*-butyl malonate. The crude crystalline residue was subjected to chromatography on silica gel eluted with ether–hexane, and the separated product was crystallized from hexane to afford 16 mg of **9**

(33) (a) Guijarro, A.; Yus, M. *Tetrahedron* **1995**, *51*, 231–234. (b) Reich, H. J.; Reich, I. L.; Yelm, K. E.; Holladay, J. E.; Gschneidner, D. J. *Am. Chem. Soc.* **1993**, *115*, 6625–6635.

(26%) as pale yellow crystals. $^1\text{H NMR}$: δ 1.53 (s, 36H), 6.63 (s, 4H), 6.76 (s, 2H). IR (KBr): 1722, 1594, 1372, 1246, 1156, 1132, 850, 800, 742 cm^{-1} . FD-MS: m/z 555 (M + 1, 80), 554 (M, 37), 57 (100). FD-HRMS for $\text{C}_{32}\text{H}_{42}\text{O}_8$: calcd 554.2880, found 554.2847. UV λ_{max} (ether): 325.5 (ϵ 28 000) nm.

Reduction of 9 with Zn in AcOH. A mixture of 21 mg of **9** (38 μmol), 126 mg of Zn powder (1.93 mmol), and 1.26 mL of AcOH was heated at 110 $^\circ\text{C}$ for 1.5 h, diluted with 15 mL of ether, washed with water ($\times 5$), and dried (MgSO_4). After the solvent was removed, the residue was subjected to preparative TLC on silica gel developed with ether–hexane (1:9) to afford 4 mg of **10** ($R_f = 0.25$, 20%) and 12 mg of **11** ($R_f = 0.11$, 57%) both as colorless crystals. **10**, $^1\text{H NMR}$: δ 1.50 (s, 18H), 1.52 (s, 18H), 2.62 (s, 4H), 6.63 (s, 4H). IR (KBr): 1722, 1630, 1372, 1286, 1250, 1156, 1134, 852, 800, 742 cm^{-1} . FD-MS: m/z 557 (M + 1, 17), 556 (M, 20), 57 (100). FD-HRMS for $\text{C}_{32}\text{H}_{44}\text{O}_8$: calcd 556.3036, found 556.3040. UV λ_{max} (ether): 235 (ϵ 12 000) nm. **11**, $^1\text{H NMR}$: δ 1.46 (s, 36H), 4.00 (s, 2H), 5.60 (s, 2H), 6.50 (s, 4H). IR (KBr): 1746, 1730, 1372, 1312, 1256, 1162, 1142, 790 cm^{-1} . FD-MS: m/z 557 (M + 1, 41), 556 (M, 100), 57 (40). FD-HRMS for $\text{C}_{32}\text{H}_{44}\text{O}_8$: calcd 556.3036, found 556.3027. UV λ_{max} (ether): 295.5 (ϵ 5600) nm.

Preparation of 12 from 6. To a solution of 13 mg of **6** (81 μmol) in 0.65 mL of CH_2Cl_2 were added successively 77 mg of *i*-Pr₂NEt (0.60 mmol) and 108 mg of *i*-Pr₃SiOTf (0.35 mmol) under argon at 0 $^\circ\text{C}$. After being stirred 26 h at 0 $^\circ\text{C}$, the resulting mixture was diluted with 10 mL of pentane, washed with water ($\times 5$), and dried (Na_2SO_4). After removal of the volatile components in vacuo, the residue was subjected to chromatography on neutral alumina eluted with benzene to afford 31 mg of **12** (82%) as a colorless oil. $^1\text{H NMR}$ (500 MHz, THF-*d*₆): δ 1.11 (d, $J = 4$ Hz, 36H), 1.15–1.25 (m, 6H), 4.59 (s, 2H), 6.60 (s, 4H). FD-MS: m/z 473 (M + 1, 41), 472 (M, 100). FD-HRMS for $\text{C}_{28}\text{H}_{48}\text{O}_2\text{Si}_2$: calcd 472.3193, found 472.3145.

Photocycloaddition of 1,4-Bis(trimethylsilyl)-2-butyne to 13. A solution of 0.89 g of **13** (6.5 mmol) and 11.8 g of 1,4-bis(trimethylsilyl)-2-butyne (60 mmol) in 160 mL of acetone was irradiated through Pyrex with a 450 W high-pressure mercury lamp under argon at -20 $^\circ\text{C}$ until **13** was largely consumed (2.5 h) and then concentrated. After the unreacted 2-butyne was recovered by distillation in vacuo (~ 100 $^\circ\text{C}$ /17 mmHg), the residue was subjected to chromatography on silica gel eluted with benzene–hexane (1:1) to afford 392 mg of **14** (18%) as a colorless oil. $^1\text{H NMR}$: δ 0.03 (s, 9H), 0.09 (s, 9H), 1.35 (d, $J = 15.6$ Hz, 1H), 1.41 (d, $J = 15.6$ Hz, 1H), 1.47 (s, 2H), 1.28–1.62 (m, 7H), 1.71 (m, 2H), 1.89 (br dd, $J = 13.2$, 9.3 Hz, 1H), 2.08 (br dd, $J = 17.6$, 7.8 Hz, 1H), 2.76 (ddd, $J = 17.6$, 12.2, 9.3 Hz, 1H). $^{13}\text{C NMR}$: δ -0.31 , 0.02, 16.22, 17.13, 20.28, 20.50, 22.48, 26.30, 31.88, 35.50, 50.09, 57.97, 138.06, 144.71, 220.39. IR (neat): 1724, 1654, 1250, 856, 846, 838, 694 cm^{-1} . FD-MS: m/z 335 (M + 1, 32), 334 (100).

Photocycloaddition of 1,4-Bis(tri-*i*-propylsilyl)-2-butyne to 13. A solution of 175 mg of **13** (1.29 mmol) and 2.36 g of 1,4-bis(tri-*i*-propylsilyl)-2-butyne in 18 mL of acetone was irradiated through Pyrex with a 450 W high-pressure mercury lamp under argon at -20 $^\circ\text{C}$ until **13** was largely consumed (10 h) and then concentrated. After the unreacted 2-butyne was recovered by distillation in vacuo (~ 120 $^\circ\text{C}$ /2 $\times 10^{-3}$ mmHg), the residue was subjected to preparative TLC on silica gel developed with benzene–hexane (1:1) to afford 21 mg of **15** (3.2%) as a colorless oil. $^1\text{H NMR}$: δ 1.06–1.09 (m, 42H), 1.39 (d, $J = 14.6$ Hz, 1H), 1.47 (d, $J = 14.6$ Hz, 1H), 1.54 (s, 2H), 1.24–1.78 (m, 9H), 1.89 (br dd, $J = 13.2$, 8.8 Hz, 1H), 2.10 (br dd, $J = 17.8$, 8.0 Hz, 1H), 2.75 (ddd, $J = 17.8$, 12.0, 9.6 Hz, 1H). $^{13}\text{C NMR}$: δ 8.94, 9.46, 12.07, 12.35, 18.98, 19.83, 20.19, 23.41, 25.06, 30.82, 36.07, 50.33, 58.82, 138.66, 146.18, 219.84. IR (neat): 1726, 1466, 882, 662 cm^{-1} . FD-MS: m/z 503 (M + 1, 35), 502 (100).

Conversion of 14 into 16. (α -Diazotization of **14**) To a mixture of 218 mg of HCO_2Et (2.95 mmol) and 160 mg of MeONa (2.96 mmol) in 2 mL of dry benzene cooled to -5 $^\circ\text{C}$ was added a solution of 197 mg of **14** (0.59 mmol) in 1.5 mL of benzene under argon. After being

stirred 17.5 h at 24 $^\circ\text{C}$, the mixture was treated with 30 mL of saturated NH_4Cl to make the mixture slightly acidic and extracted with ether (5 \times 15 mL). The ethereal extracts were combined, dried (MgSO_4), and concentrated to give 213 mg of crude α -formylated ketone as a pale yellow solid. $^1\text{H NMR}$ (90 MHz): δ 0.04 (s, 9H), 0.06 (s, 9H), 1.25–1.90 (m, 12H), 2.20 (d, $J = 14$ Hz, 1H), 2.48 (d, $J = 14$ Hz, 1H), 7.18–7.22 (m, 1H). IR (neat): 3600–2500 (br), 1690, 1666, 1598, 1250, 1182, 860, 842 cm^{-1} . FD-MS: m/z 363 (M + 1, 35), 362 (100).

To a mixture of the above crude product and 231 mg of TsN_3 (1.17 mmol) in 23 mL of CH_2Cl_2 was added 237 mg of Et_3N (2.34 mmol) at 0 $^\circ\text{C}$, and the resulting mixture was stirred for 22 h at 24 $^\circ\text{C}$ before the reaction was quenched with 17 mL of 7% KOH. After the resulting mixture was diluted with 80 mL of CH_2Cl_2 , the organic layer was separated from the aqueous layer, washed with water ($\times 3$) and brine, and dried (Na_2SO_4). After the solvent was removed, the residue was subjected to chromatography on silica gel eluted with benzene to afford 123 mg of the α -diazoketone (58% from **14**) as a reddish brown oil. $^1\text{H NMR}$: δ 0.04 (s, 9H), 0.08 (s, 9H), 1.35–1.58 (m, 5H), 1.44 (d, $J = 14.7$ Hz, 1H), 1.47 (s, 2H), 1.52 (d, $J = 14.7$ Hz, 1H), 1.65–1.80 (m, 3H), 2.63 (d, $J = 13.7$, 1H), 2.90 (d, $J = 13.7$ Hz, 1H). IR (neat): 2072, 1666, 1320, 1248, 856, 694 cm^{-1} . FD-MS: m/z 361 (M + 1, 32), 364 (100).

(Photo-Wolff rearrangement) A solution of 60 mg of the α -diazoketone (0.22 mmol) and 10 mg of Et_3N (0.10 mmol) in 4 mL of dry MeOH was irradiated through Pyrex with a 450 W high-pressure mercury lamp under argon at 5 $^\circ\text{C}$ until gas evolution ceased (3 h). After the solvent was removed in vacuo, the residue was subjected to preparative TLC on silica gel developed with benzene to afford 64 mg of the methyl ester (80%) as an ca. 9:1 mixture of stereoisomers. $^1\text{H NMR}$ (the major component): δ 0.04 (s, 9H), 0.08 (s, 9H), 1.12 (d, $J = 14.7$ Hz, 1H), 1.22–1.44 (m, 5H), 1.38 (d, $J = 14.7$ Hz, 1H), 1.46 (d, $J = 14.7$ Hz, 1H), 1.55 (d, $J = 14.7$ Hz, 1H), 1.60–1.68 (m, 1H), 1.76–1.88 (m, 2H), 1.90 (dd, $J = 12.2$, 9.8 Hz, 1H), 2.27 (dd, $J = 12.2$, 6.3 Hz, 1H), 2.93 (dd, $J = 9.8$, 6.4 Hz, 1H), 3.62 (s, 3H). IR (neat): 1738, 1644, 1448, 1436, 1250, 1200, 1170, 858, 840, 696 cm^{-1} . FD-MS: m/z 365 (M + 1, 35), 364 (100).

(α -Selenenylation of the ester) A solution of 38 mg of *i*-Pr₂NH (0.38 mmol) in 0.4 mL of THF was treated with 190 μL of 1.56 M BuLi in hexane (0.30 mmol) at -78 $^\circ\text{C}$ to afford a LDA solution, to which a solution of 54 mg of the above ester (150 μmol) in 0.4 mL of THF was added. The resulting mixture was warmed to -40 $^\circ\text{C}$ over a period of 45 min, stirred 20 min, cooled again to -78 $^\circ\text{C}$, and treated with a solution of 90 mg of PhSeBr (0.38 mmol) and 54 mg of HMPA (0.30 mmol) in 0.5 mL of THF. The mixture was warmed to room temperature over a period of 3 h, diluted with 10 mL of ether, washed with saturated NaHCO_3 ($\times 3$), and dried (MgSO_4). After the solvent was removed, the residue was subjected to preparative TLC on silica gel developed with benzene–hexane (1:1) to give 60 mg of the α -selenenylated ester (79%) as an ca. 10:1 mixture of stereoisomers. $^1\text{H NMR}$ (the major component, 90 MHz): δ 0.01 (s, 9H), 0.04 (s, 9H), 1.20–2.10 (m, 12H), 2.08 (d, $J = 13.2$ Hz, 1H), 2.87 (d, $J = 13.2$ Hz, 1H), 3.53 (s, 3H), 7.20–7.38 (m, 3H), 7.45–7.60 (m, 2H). FD-MS: m/z 522 (42), 521 (49), 520 (100), 519 (24), 518 (57), 517 (24), 516 (24).

(Conversion of the α -selenenylated ester to **16**) To a solution of 30 mg of the α -selenenylated ester (156 μmol) in 0.5 mL of CH_2Cl_2 cooled to 0 $^\circ\text{C}$ were added 20 mg of pyridine (0.26 mmol), 82 μL of water, and 82 μL of 30% H_2O_2 . The mixture was warmed to 24 $^\circ\text{C}$, stirred 2.5 h, diluted with 10 mL of ether, washed with water, saturated NaHCO_3 , and water, and dried (MgSO_4). To the ethereal solution containing MgSO_4 was added 40 μL of pyridine, and the mixture was refluxed for 2.5 h. The resulting mixture was washed with water ($\times 5$), dried (MgSO_4), concentrated, and subjected to preparative TLC on silica gel developed with benzene–hexane (1:1) to afford 28 mg of **16** (67%) as a colorless oil. $^1\text{H NMR}$: δ 0.05 (s, 9H), 0.07 (s, 9H), 1.32–1.42 (m, 4H), 1.42 (d, $J = 14.2$ Hz, 1H), 1.54 (s, 2H), 1.56 (d, $J = 14.2$ Hz,

1H), 1.83–1.90 (m, 2H), 1.90–1.98 (m, 1H), 1.99–2.08 (m, 1H), 3.76 (s, 3H), 7.31 (s, 1H). IR (neat): 1720, 1650, 1300, 1248, 1074, 856, 840 cm^{-1} . FD-MS: m/z 363 (M + 1, 38), 362 (M, 100). FD-HRMS for $\text{C}_{20}\text{H}_{34}\text{O}_2\text{Si}_2$: calcd 362.2098, found 362.2126.

Conversion of 15 into 17. (α -Diazotization of **15**) To a mixture of 87 mg of **15** (0.17 mmol) and 66 mg of HCO_2Et (0.89 mmol) in 1 mL of benzene was added 48 mg of MeONa (0.89 mmol) under argon at 5 °C. After being stirred 24 h at 24 °C, the mixture was treated with 10 mL of saturated NH_4Cl to make the mixture slightly acidic and then it was extracted with ether (5 \times 5 mL). The ethereal extracts were combined, dried (MgSO_4), and concentrated to give 55 mg of crude α -formylated ketone as a pale yellow solid. ^1H NMR: δ 0.93–1.07 (m, 42H), 1.10–1.68 (m, 12H), 2.14 (dd, $J = 15.6, 2.0$ Hz, 1H), 2.38 (d, $J = 15.6$ Hz, 1H), 7.08 (br s, 1H), 7.16 (s, 1H). IR (Nujol): 3600–2600 (br), 1668, 1600, 1162, 1120, 1070, 882 cm^{-1} . FD-MS: m/z 531 (M + 1, 45), 530 (100).

To a mixture of the above crude product and 40 mg of TsN_3 (0.20 mmol) in 4 mL of CH_2Cl_2 was added 42 mg of Et_3N (0.42 mmol) at 0 °C, and the mixture was stirred for 24 h at 24 °C before quenching the reaction with 3 mL of 7% KOH. The resulting mixture was diluted with 20 mL of CH_2Cl_2 , and the organic layer separated from the aqueous layer was washed with water ($\times 3$) and brine, and dried (Na_2SO_4). After the solvent was removed, the residue was subjected to preparative TLC on silica gel developed with ether–hexane (1:19) to afford 29 mg of the α -diazoketone (55% from **15**) as a reddish brown oil. ^1H NMR: δ 1.08 (br s, 42H), 1.20–1.85 (m, 8H), 1.48 (d, $J = 14$ Hz, 1H), 1.50 (d, $J = 15$ Hz, 1H), 1.51 (d, $J = 15$ Hz, 1H), 1.60 (d, $J = 14$ Hz, 1H), 2.69 (d, $J = 13.7$, 1H), 2.93 (d, $J = 13.7$ Hz, 1H). ^{13}C NMR: δ 8.60, 8.93, 11.94, 12.11, 18.86, 19.02, 24.42, 28.42, 30.23, 58.07, 60.94, 66.77, 140.86, 144.57, 201.08. IR (neat): 2072, 1666, 1464, 1322, 1188, 1178, 1014, 918, 882, 662 cm^{-1} . FD-MS: m/z 529 (M + 1, 48), 528 (100).

(Photo-Wolff rearrangement) A solution of 29 mg of the α -diazoketone (55 μmol) in 1.2 mL of Me_2NH was irradiated through Pyrex with a 450 W high-pressure mercury lamp for 6 h under argon at –20 °C. The resulting mixture was concentrated and subjected to preparative TLC on silica gel developed with ether–hexane (1:1) to afford 19 mg of carboxamide (66%) as a stereochemically nearly homogeneous, colorless oil. ^1H NMR: δ 1.08 (br s, 36H), 1.04–1.18 (m, 6H), 1.21 (d, $J = 14.5$ Hz, 1H), 1.22–1.78 (m, 7H), 1.58 (s, 2H), 1.68 (d, $J = 14.5$ Hz, 1H), 1.86 (dd, $J = 11.7, 9.8$ Hz, 1H), 2.05 (m, 1H), 2.49 (dd, $J = 6.4, 11.7$ Hz, 1H), 2.86 (s, 3H), 2.99 (s, 3H), 3.05 (dd, $J = 9.8, 6.4$ Hz, 1H). ^{13}C NMR: δ 8.83, 9.40, 12.09, 12.16, 18.89, 18.97, 19.15, 19.22, 21.78, 21.82, 29.52, 31.95, 32.17, 35.37, 37.27, 42.34, 43.05, 49.25, 137.95, 144.42, 173.21. IR (neat): 1730, 1652, 1466, 1392, 1150, 882, 660 cm^{-1} . FD-MS: m/z 546 (M + 1, 47), 545 (100).

(α -Selenenylation of the carboxamide) A solution of 129 mg of *i*-Pr₂NH (1.28 mmol) in 0.7 mL of THF was treated with 0.64 mL of 1.56 M BuLi in hexane (1.00 mmol) at –78 °C to afford a LDA solution, to which a solution of 57 mg of the above amide (0.10 mmol) in 1 mL of THF was added. The resulting mixture was warmed to –40 °C over a period of 1 h, stirred 3 h, cooled again to –78 °C, and treated with a solution of 302 mg of PhSeBr (1.28 mmol) and 179 mg of HMPA (1.00 mmol) in 1 mL of THF. The mixture was warmed to room temperature over a period of 3 h, diluted with 10 mL of ether, washed with saturated NaHCO_3 ($\times 3$), and dried (MgSO_4). After the solvent was removed, the residue was subjected to preparative TLC on silica gel developed with ether–hexane (3:7) to give 22 mg of the α -selenenylated amide (31%). ^1H NMR (the major component): δ 1.12 (br s, 42H), 1.20–2.20 (m, 12H), 2.47 (d, $J = 13.5$ Hz, 1H), 2.78 (s, 3H), 3.07 (s, 3H), 3.36 (d, $J = 13.5$ Hz, 1H), 7.1–7.4 (m, 5H). FD-MS: m/z 703 (36), 702 (53), 701 (100), 700 (29), 699 (57), 698 (24), 697 (19).

(Conversion of the α -selenenylated amide to **17**) To a solution of 18 mg of the α -selenenylated amide (20 μmol) in 1.5 mL of CH_2Cl_2 cooled to –78 °C was added 185 μL of 0.12 M *m*CPBA (22 μmol) in

CH_2Cl_2 . The mixture was stirred 30 min at –78 °C, treated with 20 mg of Et_3N (0.20 mmol), warmed to room temperature over a period of 2 h, and stirred 3 h. The resulting mixture was diluted with 10 mL of CH_2Cl_2 , washed with saturated NaHCO_3 ($\times 2$) and brine, dried (MgSO_4), and filtered. To the filtrate was added 0.10 mL of pyridine, and the mixture was refluxed for 6 h. The resulting mixture was washed with saturated NaHCO_3 ($\times 5$), dried (MgSO_4), concentrated, and subjected to preparative TLC on silica gel developed with ether–hexane (3:7) to afford 6 mg of **17** (60%) as a colorless oil. ^1H NMR (500 MHz, CD_2Cl_2 , 23 °C): δ 1.00–1.20 (m, 36H), 1.32–1.46 (m, 6H), 1.48–1.72 (m, 4H), 1.83–2.08 (m, 8H), 3.03 (s, 6H), 6.62 (s, 1H); (–60 °C) δ 0.90–1.15 (m, 36H), 1.18–1.38 (m, 6H), 1.44 (d, $J = 15$ Hz, 1H), 1.56 (d, $J = 15$ Hz, 1H), 1.59 (s, 2H), 1.75–1.92 (m, 8H), 2.92 (s, 3H), 3.07 (s, 3H), 6.59 (s, 1H). FD-MS: m/z 544 (M + 1, 50), 543 (M, 100). FD-HRMS for $\text{C}_{33}\text{H}_{61}\text{ONSi}_2$: calcd 543.4291, found 543.4266.

Photolysis of the Dewar Benzene Derivatives and Measurement of Electronic Absorption Spectra of [4]Paracyclophanes. A 1:1 mixture of ether and 2-methylbutane was used as solvent unless otherwise indicated. A solution of Dewar benzene precursor in 5 mL of solvent was placed in a quartz cuvette and degassed by freeze–pump–thaw cycles. After the cuvette was sealed under vacuum, the solution was frozen in liquid nitrogen to give a clear colorless glass and irradiated with a light source of specified wavelength.

(a) **Photolysis of 4.** Irradiation of a 0.9 M solution of **4** with 254 nm light led to the development of an absorption with λ_{max} 330 and 410 nm (relative intensity: ca. 3:2), which was efficiently bleached upon secondary irradiation with >400 nm light to restore the original spectrum. The species generated by the irradiation of 254 nm light was also thermally highly labile and had suffered complete decomposition when the glass was thawed below –120 °C and immediately refrozen in liquid nitrogen. On the basis of these observations, the absorption was assigned to **23**. The absorption ceased to grow in a short time of irradiation, and the extended irradiation led to the formation of second product which was stable thermally as well as photochemically and exhibited an absorption with λ_{max} 255 and 335 nm. This absorption was similar in shape to that reported for **26**³⁴ and was accordingly assigned tentatively to **26**.

(b) **Photolysis of 6.** Irradiation of a 0.3 M solution of **6** in EPA (a 5:5:2 mixture of ether, pentane, and ethanol) with 254 nm light led to the slow development of an absorption with λ_{max} 260 and 300 nm (relative intensity: ca. 3:1), which remained unchanged when the resulting glass was irradiated with 365 nm light or thawed and warmed to room temperature and, thus, appeared incompatible with the corresponding [4]paracyclophane. In a separate experiment, a solution of 5 mg of **6** in 6 mL of EPA was degassed and frozen in liquid nitrogen. After repeating an irradiation (254 nm)–thaw–freeze cycle several times, the resultant mixture was analyzed with ^1H NMR and UV. These spectra indicated the formation of **20**³⁵ in $\geq 60\%$ yield as a single detectable product. ^1H NMR (90 MHz): δ 3.90 (s, 4H), 7.70–7.80 (m, AA'XX', 2H), 8.00–8.10 (m, XX' part of AA'XX', 2H).

(c) **Photolysis of 7.** Irradiation of a 5 mM solution of **7** with 254 nm light led to development of an absorption with λ_{max} 327 and 440 nm (relative intensity: ca. 1:1), which was efficiently bleached upon secondary irradiation with >440 nm light. Difference spectra for the initial and secondary irradiation demonstrated that **7** was regenerated at the expense of the product upon the secondary irradiation, and, thus, the developed absorption was assigned to **18**. The absorption remained unchanged indefinitely at 77 K in the dark, but decayed with a half-life of 10 ± 3 min at –90 °C. The extended irradiation with 254 nm

(34) (a) Singh, I.; Ogata, R. T.; Moore, R. E.; Chang, C. W. J.; Scheuer, P. J. *Tetrahedron* **1965**, *24*, 6053. (b) Anderson, L. C.; Roedel, M. J. *J. Am. Chem. Soc.* **1945**, *67*, 955.

(35) (a) Cooper, M. A.; Manatt, S. L. *J. Am. Chem. Soc.* **1970**, *92*, 1605–1614. (b) Pearson, M. S.; Jensky, B. J.; Greer, F. X.; Hagstrom, J. P.; Wells, N. M. *J. Org. Chem.* **1978**, *43*, 4617–4622.

light led to the formation of the second product, which was thermally stable and exhibited an absorption with λ_{max} 323 nm. In a separate experiment, a solution of 4 mg of **7** in 5 mL of ether–2-methylbutane (1:1) was degassed and frozen in liquid nitrogen. After an irradiation (254 nm)–thaw–freeze cycle was repeated several times, the resultant mixture was analyzed with ^1H NMR and UV, which showed the formation of **21** as a single detectable product. ^1H NMR (90 MHz): δ 3.21 (s, 4H), 7.75–7.85 (m, AA' part of AA'XX', 2H), 8.25–8.35 (m, XX' part of AA'XX', 2H).

(d) Photolysis of 8. Irradiation of a 0.5 mM solution of **8** with 365 nm light led to the development of a broad absorption band in the range 280–410 nm at the expense of **8**. The process was reversed upon secondary irradiation with >400 nm light as demonstrated by the difference spectra recorded for the initial and secondary irradiation. The newly developed absorption decayed with a half-life of 12 ± 2 min at -20 °C. The generated species was confirmed as **24** by the ^1H NMR measurement described below.

(e) Photolysis of 10. Irradiation of a 2 mM solution of **10** with 254 nm light led to the development of absorption bands at 289, 352, and 428 nm. The latter two bands were bleached upon secondary irradiation with >400 nm light, while the band at 289 nm remained intact. Difference spectra recorded for the initial and secondary irradiation showed that **10** was regenerated at the expense of the product exhibiting the bands at 352 and 428 nm, to which structure **19** was thus assigned. The absorption due to **19** decayed with a half-life of 30 ± 5 min at -20 °C. The absorption due to **19** ceased to grow at ca. 3% conversion, and the continued irradiation with 254 nm light led to continuous growth of the band at 289 nm. The second product was stable thermally as well as photochemically and was tentatively assigned structure **22**.

(f) Photolysis of 12. Irradiation of a 15 mM solution of **12** with 313 nm light led to the development of an absorption with λ_{max} 269, 278 (sh), and 360 nm (relative intensity: ca. 10:9:1), which was efficiently bleached upon secondary irradiation with >340 nm light. Difference spectra recorded for the initial and secondary irradiation demonstrated that **12** was regenerated at the expense of the photoproduct upon the secondary irradiation. Thus, structure **29** was assigned to the latter. The absorption due to **29** decayed with a half-life of 30 ± 5 min at -50 °C. The absorption ceased to grow at ca. 2% conversion, and the continued irradiation with 313 nm light induced decomposition of **12/29** to an unidentifiable mixture.

(g) Photolysis of 16. Irradiation of a 15 mM solution of **16** with 254 nm light led to the development of an absorption with λ_{max} 302,

340, 380 (sh), and 450 nm (relative intensity: ca. 8:3:2.5:1), which was cleanly bleached upon secondary irradiation with >470 nm light to restore the original spectrum. The photoreaction of **16** reached a quasi-photostationary state at ca. 15% conversion. On the basis of this photoreversibility and similarity of the spectrum in shape to that of **33** reported previously, the developed absorption was assigned to **31**. The species was thermally unstable and suffered decomposition with a half-life of 20 ± 5 min at -130 °C.

(h) Photolysis of 17. Irradiation of a 20 mM solution of **17** with 254 nm light led to the development of an absorption with λ_{max} 302 and 390 nm (relative intensity: ca. 3:1), which was cleanly bleached upon secondary irradiation with >440 nm light to restore the original spectrum. The photoreaction of **17** reached a quasi-photostationary state at ca. 5% conversion. On the basis of this photoreversibility, the developed absorption was assigned to **32**. The absorption decayed with a half-life of 100 ± 10 min at -50 °C.

Measurement of the ^1H NMR Spectrum of 24. A solution of **8** (ca. 2 mg) in 0.6 mL of CD_2Cl_2 was placed in a Pyrex NMR tube and degassed by freeze–pump–thaw cycles. The tube was sealed under vacuum and connected to a mechanical stirrer to be rotated during irradiation. The ^1H NMR spectrum (400 MHz) recorded at -75 °C after irradiating the sample with 365 nm light at ca. -90 °C exhibited two new signals at δ 5.85 and 7.97 with an intensity ratio of ca. 2:1, besides the signals due to **8** at δ 6.93 and 7.20. The intensities of the former signals ceased to increase at ca. 6% conversion. Upon subsequent irradiation with a >400 nm light source, the signals due to the product cleanly decayed to restore the original two line spectrum.

Acknowledgment. This research was supported by Grant-in-Aids for Scientific Research (06453031 and 08454192) from the Ministry of Education, Science, Sports, and Culture of Japan. This paper is dedicated to Emeritus Professor Soichi Misumi on the occasion of his 77th birthday.

Supporting Information Available: Absolute energies and Cartesian coordinates specifying the positions of atoms for geometry-optimized **8**, **24**, and **34** at the B3LYP/6-31+G* level of theory (PDF). This material is available free of charge via the Internet at <http://pubs.acs.org>.

JA021206Y